

Continuum electron intramolecular outscattering from bare MeV/u H and He projectiles traversing hydrocarbon gases

J. E. Gaiser, J. M. Joyce, and G. Bissinger

Physics Department, East Carolina University, Greenville, North Carolina 27834-4353

(Received 23 September 1985)

The relative yields per carbon atom of continuum electrons captured by 0.6–2.5-MeV/u H⁺ and 0.5–0.8-MeV/u He²⁺ projectiles from gaseous hydrocarbon targets are observed to decrease with increasing numbers of carbon atoms and with decreasing projectile velocity. For isotachic H⁺ and He²⁺, the relative yields are the same. Assuming *intramolecular* electron-outscattering processes, additivity failure in electron capture to the continuum and its dependence of the projectile energy and molecular size can be reproduced by incorporating electron-scattering cross sections into a geometrical outscattering model.

The assumption of atomic cross-section additivity to obtain molecular cross sections, introduced in 1905 by Bragg and Kleeman,¹ has enjoyed a pragmatic acceptance that is probably based on the dual, though weak, foundations of (i) nonexistent theoretical calculations for most atomic collision processes on most molecules and (ii) some experimental evidence for its approximate validity for certain projectiles, in certain velocity regimes, and for certain molecules. This Bragg additivity rule has been used for a wide range of phenomena even though deviations have been observed for such diverse quantities as cross sections for photoionization,² Auger-electron production,³ x-ray production,^{4,5} and electron capture to bound states (ECB),^{6,7} as well as in stopping powers of compounds.⁸

Recently some of us published the results of experimental measurements of additivity failure in ECB processes with MeV/u H projectiles on hydrocarbon (C_mH_n) gas targets.⁷ These measurements had significantly improved relative precision over earlier work and exposed small, systematic deviations from "strict" additivity as both molecule size and projectile energy were varied. By estimating the effect that placing an atom in a molecule has on ECB cross sections and by incorporating *intramolecular* electron-loss processes as part of the overall electron transfer collision, it was possible to understand quantitatively the trends and magnitude of the observed departures from additivity. Further work on ECB processes with such molecules as SF₆, CO₂, and C₄F₈ led to a generalized geometrical model that used electron-loss cross sections to provide quantitative estimates of additivity failure in total electron-capture cross sections for all these molecules.⁹ In this work we present the results of a similar investigation into the validity of the additivity assumption for electron capture to the continuum (ECC) for MeV/u H⁺ and He²⁺ on *m* = 1–7 hydrocarbons.

The experimental setup utilized well-collimated H⁺ or He²⁺ beams passing through a windowless gas cell, and subsequently through a spherical sector electron analyzer placed at 0°. The entrance aperture of the electron analyzer subtended a half-angle of 3.0°. The plate voltages for the electron analyzer were stepped by a computer-controlled bipolar power supply, and the

analyzed electrons were detected by a channel electron multiplier. Gas pressure was measured in the gas cell with a 0–1-torr capacitance manometer and was regulated by a feedback-controlled valve to within better than 2%. The target gas pressures used in this experiment varied from 5 to 40 millitorr. In all cases measurements were taken in the linear portion of the gas-pressure versus continuum-electron-yield curve to ensure that all data was collected under single- (*intermolecular*) collision conditions. A typical spectrum is shown in Fig. 1. With no gas in the gas cell an external gas bleed, used to simulate the effect of charge transfer outside the gas cell, was adjusted to give the same ionization gauge reading in the chamber. The background spectrum acquired under these conditions, also shown in Fig. 1, was subtracted from the continuum-electron spectrum acquired when the gas cell was in use. Continuum-electron spectra collected at 0° form a cusp with a peak where the electron velocity *v_e* equals the projectile velocity *v_p*. Cusp spectra acquired for various C_mH_n targets with H⁺ (Ref. 10) and He²⁺ (Ref. 11) projectiles have been published previously.

Relative continuum-electron yields, derived from the cusp-electron intensities, normalized to gas pressure and accumulated charge, were examined for departures from additivity by examining the ratio, *R_c*, defined as

$$R_c = \frac{Y_c(C_m H_n)}{m Y_c(CH_4)} \approx \frac{Y_c(C_m)}{m Y_c(C)}, \quad (1)$$

where *Y_c*(C_mH_n) is the cusp-electron yield for the hydrocarbon gas under investigation and *Y_c*(CH₄) is the cusp-electron yield for methane. *Y_c*(C_mH_n) was obtained by summing the number of counts per channel in the electron energy range 0.67–1.33 times the energy of the peak in the electron spectrum. For the cusp in Fig. 1, this is from channel 36 to 72. As was the case for ECB processes⁹ this ratio showed no experimentally significant variation if the number of hydrogen atoms, *n*, in a molecule with *m* carbon atoms is varied, due to the very small cross section

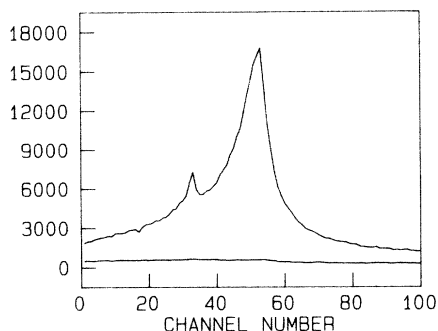


FIG. 1. A typical continuum electron energy spectrum for 0.6-MeV protons on CH_4 . A background spectrum (no gas in gas cell) taken with the chamber bled to the same background gas pressure as the cusp spectra is also shown. Note the offset of the vertical axis. The peak in channel 35 results from the C K Auger electrons.

for ECC from hydrogen as compared to carbon in our projectile energy range. In this sense, the hydrocarbon molecule acts as a "homonuclear" molecule and hence $R_c \neq 1$ is a clear indicator of additivity failure.

Experimental values of R_c calculated from our relative yields versus projectile energy (in MeV/u) are shown in Fig. 2 for $m = 2, 3, 4, 5,$ and 7 hydrocarbons. The behavior of R_c as observed from our experimental results can be summarized as follows.

- (1) For H^+ and He^{2+} , R_c decreases with decreasing projectile energy.
- (2) For a fixed-energy projectile, R_c decreases with increasing m values.

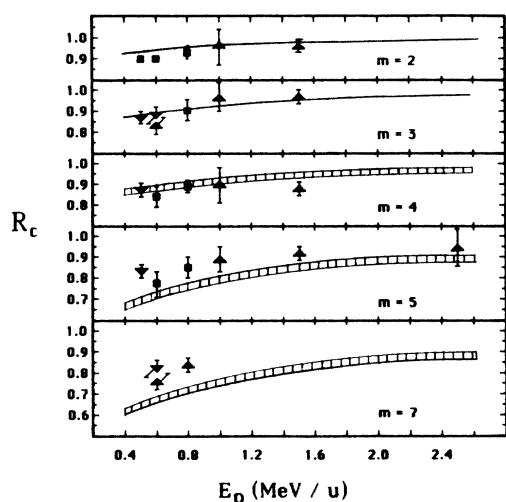


FIG. 2. Relative yield R_c [calculated from Eq. (1)] vs projectile energy E_p for H^+ (\blacktriangle) and He^{2+} (\blacktriangledown) on $m = 2, 3, 4, 5,$ and 7 hydrocarbon gases. When the H^+ and He^{2+} data coincide a (\blacksquare) symbol is used. The curves are geometrical outscattering model predictions of R_c [estimated from Eq. (4)] using total electron-scattering cross sections. The band shown for $m \geq 4$ arises from varying methods of estimating interatomic distances in these molecules.

(3) R_c is the same for equal velocity H^+ and He^{2+} . This behavior for R_c is consistent with that observed for the analogous quantity in our prior ECB work.^{7,9} Previously, we had treated the problem of additivity failure by separating the effects of the molecular environment on the molecular ECB cross sections into "entrance" and "exit" effects.⁷ Entrance effects originated from the altered electron orbital populations and binding energies due to the atom's presence in the molecule. These were estimated to lead to changes in the ECB cross sections of less than 2%—a reasonable result considering that the predominant contribution to ECB capture processes comes from the C K shell which is essentially unaffected by the chemical bonding in the outer, valence shell. Similarly, the entrance effect should be negligible for ECC processes also. Hence the departures from additivity that we observe here arise mainly from the exit effect, viz., intramolecular interactions.

Following the same general approach as in our previous work we have estimated the magnitude of intramolecular electron-scattering processes which would cause the continuum electron to be lost from the integrated cusp region. For these estimates we employ a geometrical outscattering (GO) model⁹ (used previously, e.g., by Matthews and Hopkins¹² in computing intramolecular collision probabilities for Auger electrons from molecules). This model explicitly incorporates the relevant molecular structure and atomic separations.^{13,14}

Since we are dealing with an electron in a projectile continuum state, it is assumed that any interaction that will destroy the vector velocity match between the two particles will deplete the number of electrons with $v_e \sim v_p$ collected at 0° . It is reasonable then to choose as the scattering cross sections for the GO model the total scattering cross section of electrons from carbon and hydrogen, $\sigma_{\text{tot}} = \sigma_{\text{el}} + \sigma_{\text{inel}}$, whereas for ECB additivity failure the relevant choice was electron-loss cross sections. Due to the paucity of experimental or theoretical σ_{tot} values for electrons in the 300–1500-eV range on most of the hydrocarbon gases used here, estimated σ_{tot} values were extracted from the available experimental data on $\text{CO}, \text{N}_2, \text{H}_2,$ and O_2 .¹⁵

If the cross section for electron scattering from a molecule is the sum of the cross sections for scattering from the constituent atoms, then the additivity equation for ECC from a hydrocarbon molecule can be written⁹

$$\sigma(\text{C}_m \text{H}_n) = mT(\text{C}; mn)\sigma_c(\text{C}) + nT(\text{H}; mn)\sigma_c(\text{H}), \quad (2)$$

where $T(\text{C}$ or $\text{H}; mn)$ is a quantity which we call the transmission fraction. This quantity represents the probability that a projectile-electron pair will *not* undergo an "outscattering" interaction while still in the molecule. If strict additivity of ECC cross sections were valid, then $T(\text{C}$ or $\text{H}; mn)$ would always equal 1. While it is true that strict additivity is approximately achieved for the smallest molecules at the highest projectile velocities, numerical values for the transmission fractions [calculated from the GO model with the assumption of hard-sphere scattering between a point electron, captured to the continuum from atom i and outscattered by atom j , of "radius" $(\sigma_{\text{tot}}/\pi)^{1/2}$, at an internuclear distance d_{ij}] are quite close

to 1 under these conditions also. The transmission fractions were estimated from the following equation:⁹

$$T(\text{C or H}; mn) = 1 - \frac{1}{2} \sum_{i,j} [1 - d_{ij} / (d_{ij}^2 + \sigma_{\text{tot}}/\pi)^{1/2}] . \quad (3)$$

The transmission fraction must be calculated for ECC from each atomic site in a molecule, allowing for an interaction with any other atom in the molecule. No adjustable parameters were needed in Eq. (3) to achieve good fits to the experimental data, whereas in the ECB data it was found necessary to scale the outscattering electron-loss cross sections.⁹ Calculated transmission fractions for CH₄ were 0.84, 0.89, 0.93, and 0.94 at 0.5, 0.8, 1.5, and 2.0 MeV/u, respectively. Of course the transmission fractions for the other molecules were lower, dropping to 0.53 for C₇H₁₆ at 0.5 MeV/u.

Naturally there still remains an inconsistency in our computations of the transmission fraction, viz., that we have used σ_{tot} values estimated from diatomic molecules to obtain the "atomic" cross sections used to calculate the transmission fractions. It is evident that further measurements of σ_{tot} on various hydrocarbons would somewhat improve the consistency of these calculations and permit a break out of this additivity assumption loop.

An instructive simplification occurs in the calculation of R_c from Eq. (1) if we substitute Eq. (2) into Eq. (1) and use the fact that $\sigma_c(\text{H}) \ll \sigma_c(\text{C})$ for ECC (as well as ECB) processes in our energy range, viz.,

$$R_c \simeq \frac{T(\text{C}; mn)}{T(\text{C}; 14)} . \quad (4)$$

Equation (4) can thus be compared directly to the experimental ratio, R_c , from Eq. (1) by using computed transmission fractions for each of the hydrocarbon gases at each projectile energy.

These GO model predictions of R_c are shown in Fig. 2 along with the experimental data for the bare H and He projectiles. With the transmission fractions for CH₄ given above, transmission fractions for each of the molecules

can be extracted from Fig. 2 via Eq. (4). Since the GO model predictions are sensitive only to projectile velocity, not to projectile Z (assuming insignificant entrance effects), the R_c predictions are the same for all isotachic projectiles; this prediction is consistent with our experimental R_c values for isotachic H and He, which always agreed within experimental errors.

The GO model reproduces the experimental R_c data well over the velocity range and molecular sizes covered in this experiment. The GO model predictions for $m = 4, 5,$ and 7 are presented as a band in Fig. 2 because an approximation was used to calculate the interatomic distances for any alkane (C_{*m*}H_{2*m*+2}) molecule¹⁴ of any size. This calculation was compared to the $m = 4$ alkane calculation based on accurate atomic positions¹³ and was observed to fall slightly low. The upper limit of the predictions is the calculated R_c value for the actual molecular geometry while the lower limit is based on this "alkane-string" approximation.

Interestingly, these same calculations, applied to R_c values obtained with He⁺ projectiles (not shown), do not reproduce the experimental data well at all. It is questionable whether GO model calculations of this type are even suitable for "clothed" projectiles because of the additional complication of electron-loss-to-the-continuum processes.

In summary, a geometrical model of intramolecular electron scattering with no adjustable parameters, employing total electron-scattering cross sections, gives excellent agreement with experimental relative ECC yields for \sim MeV/u bare H and He projectiles, and appears to signal the importance of intramolecular outscattering processes in ECC as well as ECB processes. While some of the agreement is no doubt fortuitous, due to the simplicity of the model, it is clear that these calculations do reproduce the experimental trends observed for ECC from hydrocarbon gases by bare MeV/u H and He projectiles.

We wish to thank Mr. Alan Larkins for his assistance in taking the data.

¹W. H. Bragg and R. Kleeman, *Philos. Mag.* **10**, S318 (1905).

²R. D. Deslattes, *Acta Crystallog. Sect. A* **25**, 89 (1969); D. F. Jackson, *Nucl. Instrum. Methods* **193**, 387 (1982).

³R. P. Chaturvedi, D. J. Lynch, L. H. Toburen, and W. E. Wilson, *Phys. Lett.* **61A**, 101 (1977).

⁴K. G. Harrison, H. Tawara, and F. J. de Heer, *Chem. Phys. Lett.* **14**, 285 (1972).

⁵G. Bissinger, J. M. Joyce, J. A. Tanis, and S. L. Varghese, *Phys. Rev. Lett.* **44**, 241 (1980).

⁶A. B. Wittkower and H. D. Betz, *J. Phys. B* **4**, 1173 (1971).

⁷G. Bissinger, J. M. Joyce, G. Lapicki, R. Laubert, and S. L. Varghese, *Phys. Rev. Lett.* **49**, 318 (1982).

⁸J. W. Wilson, C. K. Chang, Y. J. Xu, and E. Kameratos, *J. Appl. Phys.* **53**, 828 (1982); W. Brandt, in *Proceedings of the Workshop on Current Stopping Power Problems*, New York, January, 1978, Summary Report (unpublished).

⁹S. L. Varghese, G. Bissinger, J. M. Joyce, and R. Laubert, *Phys. Rev. A* **31**, 2202 (1985).

¹⁰G. Bissinger, J. Gaiser, and J. M. Joyce, *IEEE Trans. Nucl. Sci.* **NS-30**, 1015 (1983); G. Bissinger, *Nucl. Instrum. Methods* **214**, 81 (1983).

¹¹G. Bissinger, J. Gaiser, J. M. Joyce, and M. Numan, *Phys. Rev. Lett.* **55**, 197 (1985); G. Bissinger, *Nucl. Instrum. Methods B* **10**, 271 (1985).

¹²D. L. Matthews and F. Hopkins, *Phys. Rev. Lett.* **40**, 1326 (1978).

¹³L. C. Snyder and H. Basch, *Molecular Wave Functions and Properties* (Wiley, New York, 1972).

¹⁴R. Hoffman, *J. Chem. Phys.* **39**, 1397 (1963).

¹⁵B. L. Jhanwar, S. P. Khare, and M. K. Sharma, *Phys. Rev. A* **26**, 1392 (1982); G. Dalba *et al.*, *J. Phys. B* **13**, 4695 (1980); B. van Winderghen, R. W. Wagenaar, and F. J. deHeer, *ibid.* **13**, 3481 (1980); W. E. Kauppila *et al.*, *Phys. Rev. A* **24**, 725 (1981); H. J. Blaauw, R. W. Wagenaar, D. H. Barends, and F. J. deHeer, *J. Phys. B* **13**, 359 (1980).